ºA Novel [Os(1,10-phenanthroline-5,6-dione)$_2$(PVP)$_4$Cl]Cl Redox Polymer for Electrocatalytic Oxidation of NADH and its Application to the Construction of Reagentless β–D-glucose Biosensors

Valeri Pavlov,[1] Óscar Rincón,[2] Sonia Solé,[1] Arantzazu Narváez,[2] Elena Domínguez,[2] Ioanis Katakis[*1]*

Bioanalysis and Bioelectrochemistry Group, Chemical Engineering, Universitat Rovira i Virgili, E-43006, Tarragona (Catalonia), Spain, and Departamento de Química Analítica, Universidad de Alcalá, E-28871 Alcalá de Henares (Madrid), Spain.

RECEIVED DATE

[*] To whom the correspondence should be addressed. E-mail: ioanis.katakis@urv.net**,** Tel: +34 977 55 9655. Fax: +34 977 55 9667.

[1]Universitat Rovira i Virgili.

[2]Universidad de Alcalá.

ABSTRACT. The synthesis and study of the electrochemical behaviour of [Os(1,10-phenanthroline-5,6-dione)2-poly(4-vinylpyridine)4Cl]Cl redox polymer are reported. With cyclic voltammetry in aqueous phosphate buffer solutions at different scan rates and pH values, it was found that in aqueous solutions four protons and four electrons participate in the redox cycling of o-quinone (phendione) and the rate constant for the heterogeneous electron transfer of the phendione redox couple kS is equal to 18±2 s-1 at pH 6.0. The electrocatalytic oxidation of β-nicotinamide adenine dinucleotide (NADH) at graphite rotating disk electrodes modified with this redox polymer was studied and the second order rate constants for NADH oxidation $k_{[NADH]=0}$ were determined to be $(1.9\pm0.2)x10^3$ $M^{-1}s^{-1}$ at pH 6.0 and $(3.4\pm0.3)x10^3$ $M^{-1}s^{-1}$ at pH 5.0. This novel electroactive polymer was used for the construction of reagentless glucose biosensors whereby NAD^+ and glucose dehydrogenase were immobilized on the graphite electrode surface. Such sensors showed operational lifetimes limited by leaching of NAD^+.

KEYWORDS. glucose analysis, thermophilic, glutamate dehydrogenase, reagentless biosensors, NAD^+.

More than 300 enzymes[1] use β-nicotinamide adenine dinucleotide (NAD^+) as a cofactor and therefore the development of methods for electrocatalytic oxidation of NADH attracts a great deal of theoretical and practical interest due to the possibility of applications to the design of biosensors, bioreactors and fuel cells. Despite the fact that the reversible potential for NADH/NAD^+ couple is -0.56 V *vs*. SCE[3] direct electrooxidation of NADH at bare electrode surfaces is not convenient because it is not chemically reversible and requires high overpotentials.[3]

Different strategies to accelerate the kinetics of NADH oxidation were critically examined in comprehensive works,[4,5] modification of the electrode surface being one of them. First attempts to carry out such modification include an electrochemical pretreatment of carbon electrodes leading to the formation of surface hydroxyl and quinone groups.[6] Another set of methods relies on covalent binding and adsorption on the electrode surface of different mediators for NADH oxidation such as *ortho*- and *para*- quinines,[7,8] *ortho*- and *para*-phenylenediimines,[9-10] organic conducting salts,[11] hydroxysubstituted

phenoxazine,[12] metal complexes containing *o*-quinone ligands.[13,14] The electrodes modified with small molecules usually suffer from low surface coverage and leaching of the mediator to a bulk solution.

Modification of electrodes with redox polymers is preferable because it can decrease leaching. In addition the catalytic response of polymer-coated electrodes to NADH is much higher than this of a monolayer of immobilized small molecules since polymeric films contain the equivalent of many immobilized monomolecular layers and if all of them remain active, the number of electroactive sites is superior.[15] Three major groups of NADH oxidizing polymers have been reported in the literature.

Polymers made from electropolymerization of monomers without intrinsic mediating properties such as poly(3-methylthiophene).[16] Polymers produced by electropolymerization of monomers with intrinsic mediating properties, for example, poly(thionine),[17] poly(3,4-dihydroxybenzaldehyde).[18] Premade polymers into which mediating functionalities are covalently bound. For instance dopamine attached to poly(methacrylate),[19] Toluidine Blue O connected through various spacers to polyalkane backbones,[20] In general most polymeric mediators showed lower rate constants of oxidation of NADH than the corresponding monomers because of "capping" by the polymer backbone of the active redox sites, oriented towards the electrode surface.[21] The majority of monomeric and polymeric mediators has pH dependent redox potential and rate of interaction with NAD(P)H. Both of them increase when pH decreases because of protons participating in the redox conversion of $NAD(P)^+$/NAD(P)H couple and many mediators facilitate hydride transfer to accepting groups of mediators.

Polymeric mediators proved to adhere more than small molecules to the electrode surface, but inherit from their corresponding monomers low chemical and operational stability. Almost all reported mediators for NAD(P)H oxidation can be used in pH range from 2 to 7 and showed the increased decomposition rate at the pH above 7.0 where the majority of the known $NAD(P)^+$ dependent dehydrogenases has optimal activity. The complexes of some transition metals with 1,10-phenanthroline-5,6-dione proved to be chemically more stable and more reversible in alkaline media.

The reaction of electrochemical oxidation of NAD(P)H can be coupled with the reaction of enzymatic oxidation by dehydrogenases to yield a great number of possible configurations applicable to the

construction of biosensors, bioreactors and fuel cells. Many electrodes operating in the presence of enzymes, cofactors and mediators in a sample solution have been demonstrated in the literature, but the number of dehydrogenase electrodes which can detect an analyte without addition of any additional reagent to a sample solution, so called reagentless electrodes, is limited.

The most stable biosensors were produced on the basis of a carbon paste in which a "reserve pool" of the coenzyme was created, at the same time their sensitivity was high.[22] Unfortunately, it is impossible to opt for carbon paste configurations to fabricate miniaturized sensors.

In the present work we report on an effort to produce reagentless NAD^+-dehydrogenase electrodes. For this purpose we synthesized a novel NADH oxidizing polymer [Os(1,10-phenanthroline-5,6-dione)$_2$(PVP)$_4$Cl]Cl (Os-phendione-PVP), produced by complexation of poly(4-vinylpyridine) with the complex [Os(1,10-phenanthroline-5,6-dione)$_2$Cl$_2$]. We also report on the study of the electrochemical behaviour of Os-phendione-PVP adsorbed on spectrographic graphite and on the determination of the kinetics of NADH oxidation at these electrodes. We apply Os-phendione-PVP coated electrodes to the construction of reagentless glucose biosensors using glucose dehydrogenase. Furthermore, we discuss the possible limiting steps for operational stability of such sensors.

RESULTS AND DISCUSSION

Electrochemistry of Os-phendione-PVP. The water insoluble redox polymer was produced by complexation of [Os(1,10-phenanthroline-5,6-dione)$_2$Cl$_2$] with poly(4-vinylpyridine) at an 1:4 molar ratio in ethylene glycol (Figure S-1 in Supporting Information). The previous studies of electrochemistry of free 1,10-phenanthroline-5,6-dione[13,23,24] and its complexes with metals[13,24] have shown that in a protic solvent they behave as quasi reversible, pH dependent redox couple with two-electrons and two-protons participating in the redox process per phendione moiety. Cyclic voltammetric scans of Os-phendione-PVP adsorbed on a graphite electrode, recorded in aqueous phosphate buffer (Figure 1) have demonstrated one wave with a formal redox potential ($E^{o'}$) (calculated as the average of

cathodic and anodic peaks potentials) of +38.7±0.4 mV *vs.* $Ag/AgCl/KCl_{sat}$ at the pH 6.0. For scan rate of 50 mV s^{-1} the peak-to-peak potential separation (ΔE_p) was 57.5±0.4 mV, and the ratio I_{pa}/I_{pc} was =1.1±0.1. The voltammetric waves of $Os^{II/III}$ are reversible, the formal standard potential for this redox couple is 407±2 mV as expected for the osmium atom coordinated with two phendione ligands, one pyridine ligand of PVP, and a Cl^-. Taking into consideration that this couple exchanges only one electron and comparing the peak areas for the phendione/catechol and $Os^{II/III}$ it was estimated that the number of electrons exchanged in phendione is equal to 4.0±0.1 at the pH lower than 6.4. At higher values of the pH the apparent number of electrons cycling decreased (Figure S-2 in Supporting Information), probably, because of the chemical irreversibility of phendione redox couple at pH>6.4. The stability of Os-phendione-PVP modified graphite electrodes at pH 6.0 was studied by running 50 consecutive cyclic voltammograms with the scan limits from –200 to 600 mV. At the end of this experiment the phendione peak area stabilized after having decreased by 11%, without any change in the voltammogram shape. It seems therefore that a slow desorption of the polymer occurs while the chemical stability of the redox moieties is not affected at these time scales.

The cyclic voltammetry at pH 5.0, 6.0 and 7.0 demonstrated a linear dependence of the anodic (Figure S-3 in Supporting Information) and cathodic (Figure S-4 in Supporting Information) peak currents (I_{pa} and I_{pc}) on scan rate (υ) at scan rates up to 500 mV/s. The plots of I_p versus $\upsilon^{1/2}$ were not linear at any scan rate range, suggesting that the very thin film of Os-phendione-PVP deposited on the electrodes is strongly adsorbed and there are no electron or proton diffusion processes limiting the electrochemistry. The surface coverage of Os-phendione-PVP on the graphite electrodes was $(6.7\pm 0.5)\times10^{-10}$ mol cm^{-2}.

Protons take part in the redox reaction of Os-phendione-PVP according to the following scheme:

$$Os(Q)_2PVP + 4e^- + 4H^+ \rightleftharpoons Os(QH_2)_2PVP$$

where $Os(Q)_2PVP$ and $Os(QH_2)_2PVP$ stand for oxidized and reduced forms of the ligand, respectively. This equation explains why the redox potential of phendione in the electroactive polymer must be pH dependent. The phendione's $E^{0,}$ dependence on the value of pH (Figure S-5 in Supporting Information)

was studied by recording cyclic voltammograms of electrodes modified with Os-phendione-PVP changing the pH from 3 to 8. The value of the lowest limit of the pH was selected as 3 because of NADH hydrolysis in acidic media[25] therefore the behaviour of the mediator is not of interest at pH<3 for NADH catalysis. The value of 8 for the highest pH limit was chosen due to the fact that phendione is unstable at pH values higher than 8.[23] The standard redox potential shifts in the negative direction with the increase in the solution pH (Figure S-5 in Supporting Information). Three different regression lines can be drawn for three pH intervals. Within the range of pH from 3 to 5.5 the regression line is $E^{0'}$/V=0.385-0.060pH, (r^2=0.9991; n=6), the slope is close to its theoretical value of 59 mV per pH unit, calculated for processes in which equal number of protons and electrons participate, strongly indicating that the overall reaction proceeds with the participation of equal number of electrons and protons. From pH 5.5 to 6.4 the line is $E^{0'}$/V=0.348-0.052pH, (r^2=0.9993; n=9). Knowing that the pK of pyridine in PVP is 5.5 this change of the slope can be explained in terms of deprotonation of pyridine rings. For the pH range from 6.4 to 8 the line is $E^{0'}$/V=0.327-0.049pH, (r^2=0.9994; n=7). Taking into consideration that the theoretical slope value for the redox process with the participation of four electrons and three protons is 44 mV per pH unit it can be concluded that only one of four hydroxyls in $Os(QH_2)_2$PVP complex is deprotonated in this pH range. This change in slope occurs at pH 6.4 suggesting that the pK_a of the reduced mediator has the same value. This data coincide with the value of the pK_a obtained in our previously reported electrochemical study of another complex of osmium with phendione [Os(4,4'-dimethyl-2,2'-bipyridine)$_2$(1,10-phenanthroline-5,6-dione)]$(PF_6)_2$.[14] Free 1,10-phenanthroline-5,6-dihydroquinone demonstrates the pK_a of 9.0,[23] but its complexation with divalent metals leads to the strong acid shift of the pK_a.[13] The dependence of ΔE_p on the pH (Figure S-6 in Supporting Information) reflects the dependence of the apparent heterogeneous electron transfer rate constant (k_S, s^{-1}) on the pH. It can be seen that ΔE_p increases with the pH until the pH 6.0 with the breaking point at the pH 4.5 and next at the pH 6.5. This variation of k_S with the pH corroborates with the theory developed by Laviron for organic redox couples in which protonation reactions take place .[26,27] Laviron's theory predicts the decrease in k_S with the pH. The quantitative variation of k_S and hence ΔE_P can be calculated if the

constants of all protonation reactions for all participating forms of the mediator together with k_{S1} and k_{S2} are known for the following reversible reactions insensible to pH:

$$Os(QH_2)_2PVP + 4e^- \overset{k_{S1}}{\rightleftharpoons} Os(QH_2^{2-})_2PVP$$

$$Os(Q)_2PVP + 4e^- \overset{k_{S2}}{\rightleftharpoons} Os(Q^{2-})_2PVP$$

Where $Os(QH_2)_2PVP$ is a fully protonated oxidized form and $Os(Q^{2-})PVP$ is a fully deprotonated reduced form of the mediator. Unfortunately, these constants for this mediator can not be found due to its chemical instability at pH>6.5. So only qualitative analysis of the ΔE_P *vs.* pH plot can be undertaken.

The variation of the cathodic and anodic peak potential (E_{pc} and E_{pa}) for the phendione couple with the scan rate was used to estimate the heterogeneous electron transfer rate constant (k_S, s^{-1}) of the redox process, taking place at the interface between the electrode surface and Os-phendione-PVP adsorbed on it, according to Laviron's approach:[28]

$$E_{pc}-E^{0'}=(2.303RT/\alpha nF)\log[\alpha nF\upsilon/(RTk_S) \quad (1)$$

$$E_{pa}-E^{0'}=(2.303RT/(1-\alpha)nF)\log[(1-\alpha)nF\upsilon/(RTk_S) \quad (2)$$

where υ is the scan rate (V s^{-1}), n-the number of exchanged electrons, F is Faraday's constant 96487 C mol^{-1}, and α the transfer coefficient. If the transfer rate is fast enough in comparison with the scan rate then the peak separation is close to zero and when the scan rate is greater than the transfer rate the peak separation increases. This approach is supposed to give a lower limit estimate for the value of k_S, which in the case of Os-phendione-PVP is equal to 18±2 s^{-1} at pH 6.0 (calculated as average of cathodic and anodic constants) and surface coverage (7.5±0.2)x10^{-10} mol cm^{-2}, oxidation and reduction transfer numbers being 0.86±0.05 and 0.12±0.01 at pH 6.0. The estimated apparent k_S value for this polymer is higher than this for Meldola Blue (10 s^{-1}),[9] and of the same order of magnitude as these for [Os(4,4'-dimethyl-2,2'-bipyridine)$_2$(1,10-phenanthroline-5,6-dione)]$(PF_6)_2$ (20.1 s^{-1}).[14] The sum of the anodic and

cathodic transfer coefficients is almost one, but the small asymmetry with respect to the abscissa of the anodic and cathodic lineal branches of the (E_p-$E^{0'}$) *vs*. log(υ) plot can be seen (Figure S-7 in Supporting Information). The exact numerical values of k_S could not be estimated exactly at the pH greater than 6.4 due to the chemical instability of Os-phendione-PVP nevertheless the dependence of ΔE_p on the pH allows to see the decrease of peak separation starting from this pH indicating increased reversibility upon protonation of resulting catechol.

According to theory the peak width at half peak height, E_{fwhm} depends on the reversibility of a redox couple. It should be equal to 90.6/n mV for an ideally Nernstein reversible reaction (when n = 4 E_{fwhm} should be 22.5 mV) and 62.5/(αn) for the irreversible electrochemical process (when n = 4 and α = 0.86, oxidation E_{fwhm} is 18.38 mV, for α = 0.12 reduction E_{fwhm} should be 130.2 mV). In the case of Os-phendione-PVP, E_{fwhm} was pH dependent as is shown in Table I. The values of oxidation and reduction E_{fwhm} increase with pH and are greater than those predicted by theory for reversible and irreversible processes indicating repulsing interactions between adsorbed molecules. Thus it can be concluded that Os-phedione-PVP is a quasi-reversible redox couple exchanging four protons and four electrons at pH less than 6.4.

Electrocatalytic oxidation of NADH at Os-phendione-PVP modified electrodes. Cyclic voltammograms showing electrocatalytic current due to the NADH oxidation on Os-phendione-PVP modified graphite electrodes at different NADH concentrations are shown in Figure 2. In the absence of NADH (a) the response is ascribed to the oxidation/reduction of catechol/phendione couple. Upon addition of increasing concentrations of NADH (b-d) the cyclic voltammograms exhibit a dramatic enhancement of the anodic peak current with the disappearance of the cathodic peak. The peak of the NADH oxidation at bare graphite electrodes is at 332±5 mV *vs.* Ag/AgCl/KCl_{sat}, modified electrodes show a plateau at +112±8 mV *vs.* Ag/AgCl/KCl_{sat} at pH 6.0, at scan rate of 20 mV s^{-1} with NADH concentration of 2.4 mM (curve d), which is close to the oxidation peak of adsorbed mediator itself at

the same value of pH (+53±3 mV *vs.* Ag/AgCl/KCl_{sat}). Therefore, a decrease in NADH electrooxidation overvoltage by about 220 mV compared to electrooxidation at bare graphite electrodes under the same conditions (Figure 3) is achieved with the redox polymer. Rotating disk electrodes (RDE) were used to assess the stability of the steady state signal and calculate the rate constants of NADH oxidation by Os-phendione-PVP adsorbed on graphite electrodes.

The estimation of rate constants for the reaction between NADH and Os-phedione-PVP was based on the hypothesis that in thin polymeric films diffusional transport of both charge and NADH can be neglected and the substrate-mediator complex is formed in this interaction according to the following mechanism:

$$\text{Os-phendione-PVP} + \text{NADH} \underset{k_{-1}}{\overset{k_1}{\rightleftarrows}} [\text{Os-phendione-PVP}\cdot\ \text{NADH}] \xrightarrow{k_2} \text{Os-catechol-PVP} + \text{NAD}^+$$

The model proposed by Gorton and coworkers[4,9] to calculate the dependence of the catalytic current (I_{cat}) on experimental parameters on the basis of a Michaelis-Menten kinetic model was employed in this work.

$$1/I_{cat}=1/(\mathrm{n}FA\Gamma kc_{NADH}) + [1/(0.62nFAD^{2/3}\ c_{NADH}\ \nu^{-1/6})](1/\omega^{1/2}) \quad (3)$$

$$1/I_{cat}=1/(\mathrm{n}FA\Gamma k_2) + [K_M/(nFA\Gamma k_2) + 1/(0.62nFAD^{2/3}\nu^{-1/6}\omega^{1/2})](1/c_{NADH} \quad (4)$$

$$K_M=(k_{-1}+k_2)/k_1 \quad (5)$$

where D ($cm^2\ s^{-1}$) is the diffusion coefficient of NADH, ν ($cm^2\ s^{-1}$) the hydrodynamic viscosity, ω (rad s^{-1}) the speed of rotation, A (cm^2) the electrode surface area, Γ (mol cm^{-2}) the surface coverage of the mediator, c_{NADH} (M) the concentration of NADH, and k ($M^{-1}\ s^{-1}$) the rate coefficient of the formal overall chemical reaction:

$$\text{Os-phendione-PVP} + \text{NADH} \xrightarrow{k} \text{Os-catechol-PVP} + \text{NAD}^+$$

When the data obtained from RDE measurements, were plotted as $1/I_{cat}$ against $1/\omega^{1/2}$ for different concentrations of NADH straight lines were obtained in agreement with equation 4 (Figure S-8 in Supporting Information). From the intercepts of these lines with the $1/I_{cat}$ axis the coefficients k were estimated and the graph of k^{-1} *vs.* c_{NADH} (Figure S-9 in Supporting Information) according to equation 6 was made.

$$1/k = K_M/k_2 + c_{NADH}/k_2 \quad (6)$$

On the basis of the resulting straight line (y = 0.896 + 0.9495x, R = 0.997 (n = 6)) the values of kinetic constants k_2, K_M, and $k_{[NADH]=0}$ (rate coefficient of the overall reaction at zero NADH concentration) were found at pH 6.0 and 5.0 and are summarized in Table II.

The value of K_M for the present redox polymer is equal to that of Meldola Blue (1.2 mM),[9] lower than that for [Os(4,4'-dimethyl-2,2'-bipyridine)$_2$(1,10-phenanthroline-5,6-dione)](PF$_6$)$_2$ (0.39-0.43).[14] Comparing the value of k_2 with this reported for other NAD^+ oxidizing mediators it can be seen that it is of the same order of magnitude as k_2 of [Os(4,4'-dimethyl-2,2'-bipyridine)$_2$(1,10-phenanthroline-5,6-dione)](PF$_6$)$_2$ (0.75-0.8 s^{-1})[14] and it is inferior to k_2 of Meldola Blue (31.8 s^{-1}).[9] The rate coefficient k strongly depends on the NADH concentration, for this reason is was proposed[17] to use its value extrapolated to zero NADH concentration ($k_{[NADH]=0}=k_2/K_M$), which in case of Os-phendione-PVP was lower than the corresponding value for Meldola Blue (2.7×10^4 M^{-1} s^{-1})[9] or for poly(3,4-dihydroxybenzaldehyde) (4.3×10^3 $M^{-1}s^{-1}$)[38] and practically equal to that of [Os(4,4'-dimethyl-2,2'-bipyridine)$_2$(1,10-phenanthroline-5,6-dione)](PF$_6$)$_2$ (0.9 M^{-1} s^{-1}).[14]

The construction of stable and operational NADH-based reagentless biosensors requires not only efficient electrocatalytic oxidation of NADH by the mediator but also that the electrocatalytic process yields enzymatically active NAD^+. Recycling of NADH into enzymatically active NAD^+ was carried out by electrochemical conversion experiments as described in Supporting Information. This experiment showed that 100% of the oxidation product is enzymatically active NAD^+.

Reagentless glucose biosensors constructed using Os-phendione-PVP. With an objective to prove the applicability of the redox polymer Os-phendione-PVP to the construction of dehydrogenase-based biosensors glucose dehydrogenase (GDH) was selected as a model enzyme to be used in a biosensor configuration based on NAD^+ recycling. The sequence of electrochemical reactions taking place in this biosensor is demonstrated in Figure 4. Os-phendione-PVP was used in conjunction with GDH and NAD^+ crosslinked with PEGDGE in the matrix based on the "binder" polymer. The electrocatalytic behavior of the modified electrode containing GDH and NAD^+ is shown in Figure 5. It can be observed that when D-glucose is added into the bulk solution a significant oxidation current appears associated with the disappearance of the reduction peak. Controlled electrodes have been prepared excluding one of the following components: a) NAD^+; b) Os-phendione-PVP; c) GDH; d) "binder" polymer; e) PEGDGE. None of them demonstrated any significant response to glucose. The characterization of glucose dehydrogenase from *Bacillus megaterium*, the enzyme used in this work, was reported for the first time by Pauly and Pfleiderer.[29] The free enzyme follows a Bi Bi sequential ordered mechanism taking place via the formation of a ternary complex. NAD^+ adds first and the NADH formed dissociates from the enzyme last, hence the calculations of characteristics of the glucose sensors were performed using the steady-state kinetic model published elsewhere[30] and modified as shown in Supporting Information.

Experimental calibration curves for the glucose biosensors prepared with different loadings of GDH operating in the presence of saturating 26 mM NAD^+ in the external solution were used to find the values of the apparent Michaelis constants, the apparent maximum current densities and the fluxes from the Eadie-Hofstee plots (Figure S-25 in Supporting Information). By fitting the experimental data to equation S-22 (Supporting Information) using non-linear regression analysis the values of LV_1, K_B, and k'_B were found (Table S-I in Supporting InformationI). For the meaning of LV_1, K_B, and k'_B see Supporting Information. The Eadie-Hofstee plots were linear and the values of calculated apparent Michaelis constants were practically equal when the loading of GDH was varied, at the same time the apparent maximum current densities changed linearly with the variation in the GDH loading. Fitting the

experimental calibration data gave the values of LV_l of K_B coinciding with those of the apparent maximum fluxes and the apparent Michaelis constants for glucose. The computed value of K_B agrees well with that of the free GDH in solution (9.7 mM) determined under the same experimental conditions. The computed values of the mass transfer constants of glucose (k'_B) were greater than $1x10^{-8}$ cm s^{-1} implying that in the experimental range of substrate concentrations starting from 0.047 mM the flux of the mass transfer of the substrate was not less than the maximum flux of the enzymatic reduction of NAD^+ ($4.77x10^{-10}$ mol s^{-1} cm^{-2}). Hence, the response of the glucose biosensors operating in the presence of saturating NAD^+ concentration in a sample solution is limited by the enzymatic reaction of the glucose oxidation i.e. by the GDH loading.

The experimental calibration curves and the Eadie-Hofstee plots (Figure S-26 in Supporting Information) for the biosensors prepared with varied loadings of GDH operating in the reagentless mode i.e. without NAD^+ in the sample solution yielded the values of the apparent Michaelis constants, the apparent maximum current densities and fluxes obtained from the Eadie-Hofstee plots.The Eadie-Hofstee plots were linear implying that the response of the biosensors is limited neither by the rate of NADH oxidation at the electrode surface nor by the mass transfer of glucose. The values of apparent Michaelis constants were dependent on the GDH loading and the values of the apparent current densities, and fluxes did not rise linearly with the increase in the GDH loading. Fitting the experimental calibration data to the equation S-21 in Supporting Information by non-linear regression analysis using the values of LV_l, K_B, and k'_B yielded by previous fitting allowed to assess the values of K_A, K_{AB}, and A_t (Table S-II in Supporting Information). For the meaning of K_A, K_{AB}, and A_t see Supporting Information. The values of K_A and K_{AB} were quite similar at varied NAD^+ loading but the values of the computed NAD^+ loading (A_t) decreased with the increase in GDH loading meaning that GDH competes for crosslinking by PEGDGE with the entrapment of NAD^+ in the resulting hydrogel. The decrease in maximum current densities caused by the decrease in NAD^+ concentration showed by the reagentless glucose biosensors, in comparison with the biosensors operating in the presence of NAD^+ in an external solution, proves that the response of the reagentless biosensors to glucose is limited by the enzymatic

reduction of NAD^+ i.e. by NAD^+ loading (A_t). In conclusion it should be noted that the values of K_A, and K_{AB} obtained by fitting agree well with those of free GDH in the solution under the same experimental conditions: 1.85 mM and 5.1 mM^2 respectively.

The effect of pH on the response of the glucose biosensors is demonstrated in Figure 6. One can see that the response of the biosensors increases with pH in agreement with pH behavior of free GDH from *Bacillus megaterium* reaching the maximum current at pH 9.0 which is the pH optimum of GDH. The effect of temperature on the response to glucose of the biosensors was studied. (Figure S-27 in Supporting Information). In the reagentless mode of operation the glucose biosensors demonstrated the maximum current at the temperature of 54^{o}C and in the presence of 29 mM NAD^+ in the sample solution they achieved maximum response at 66^{o}C. Free GDH has optimum temperature at 55^{o}C and shows 80% of its maximum activity at 66^{o}C. The lower thermal stability of the reagentless sensors can be explained by the increased rate of NAD^+ leaching at elevated temperatures, on the other hand the increased thermal stability, demonstrated by the immobilized enzyme in the sensors operating in the presence of the cofactor in the sample solution, is most probably a reflection of the stabilization of the enzyme proteins due to their chemical crosslinking with the hydrogel matrix. The activation energies calculated from the temperature *vs.* response plots for the reagentless and non-reagentless biosensors have the values of 54±6 kJ mol^{-1} K^{-1} and 61 ±6 kJ mol^{-1} K^{-1} respectively. They corroborate with the activation energy of free GDH (60 kJ mol^{-1} K^{-1}) measured under the same experimental conditions in the presence of 26 mM NAD^+, this fact means that at elevated temperatures the response of the glucose sensors is also governed by the enzymatic reaction of glucose with NAD^+.

The operational stability studies performed at the saturating glucose concentration (220 mM) with the sensors prepared using 0.135 U per electrode of glucose dehydrogenase demonstrated that the half-life time of reagentless biosensors is 1 h (RSD 6.4 % for three electrodes) and they lost 33% (RSD=11% for n=3) of phendione activity, when at the end NAD^+ was added to obtain saturating concentration of cofactor the current density rose to 54.1 μA cm^{-2} (60 % of the initial response in the presence of 26 mM NAD^+). Controlled biosensors operated in the absence of glucose during 1 h under the same conditions

lost 8% (RSD 10%, n=3) of the mediator. When the glucose sensors were operated in the presence of NAD^+ in the bulk solution since the beginning of experiment the operational half-life was 2.4 h (RSD=12% for n=3). Those sensors lost 56 % of phendione activity (RSD is 15% for n=3). The enzymatic measurements of NAD^+ concentration based on the spectroscopical monitoring at A_{340} of its reduction to NADH by glucose dehydrogenase showed that NAD^+ was stable in the sample solution under the experimental conditions during the at least 2.4 h. Controlled sensors lost only 28 % (RSD 13%, n=3) of the mediator after 2.4 h in the absence of glucose. The significant difference in the loss of Os-phendione-PVP between the glucose biosensors operating in the reagentless mode and those operating in the presence of NAD^+ (33% and 56 % respectively) upon reaching 50% of their initial response proves that the mediator loading is not the limiting factor for the response of the sensors to glucose. Otherwise, if the oxidation of NADH by the mediator is the limiting step, the loss of the response to glucose should be linearly dependent on the loss of the mediator. The most important reason for the deactivation of the reagentless glucose biosensors is leaching of NAD^+. This is confirmed by shorter half-life time demonstrated by the reagentless biosensors.

CONCLUDING REMARKS

A new NADH oxidizing polymer was synthesized and used for the modification of graphite electrodes by adsorption on their surface. Four protons and four electrons participate in the redox process taking place at two 1,10-phenanthroline-5,6-dione ligands complexed with osmium central cation causing pH dependent electrochemical behaviour. Although the complexation increases the relative stability of the electrocatalytic ligand, still the redox active polymer was useful at pH < 7. Work continues on the stabilization of these types of ligand to achieve faster kinetics, chemically reversible behaviour and greater stability. The reaction of the polymer with NADH proceeds reversibly through the formation of an intermediate complex, as was shown by RDE studies at different rotation velocities and NADH concentrations, when thin polymeric monolayer was immobilized on graphite. The polymer generates

enzyimatically active NAD^+ according to the conversion study. Good electrocatalytic activity of the polymer for NADH oxidation allowed to construct the reagentless glucose biosensors based on NAD^+ and glucose dehydrogenase entrapped in the hydrogel. It was confirmed that the response of the reagentless glucose biosensors is governed by the kinetics of the enzymatic reaction of glucose with NAD^+.

ACKNOWLEDGMENTS

Financial support from the European Community under the Industrial & Materials Technologies Programme Ref.: PROMOFILM BRITE EURAM Program BE97-4511, the Spanish Ministry of Education and Culture Ref.: Acciones Especiales MAT98-1413.CE, and the Biotechnology Program Ref.: DIAMONDS BIO4-CT97-2199 financed by European community is gratefully acknowledged. V.P. acknowledges scholarship from the Department of Chemical Engineering of 'Rovira i Virgili' University. O. R. and A. N. acknowledges scholarships from the Spanish Ministry of Education and Culture and the Community of Madrid, respectively. S. S. acknowledges a summer training scholarship from the PROMOFILM project.

Supporting Information Available. Additional information as noted in text. This material is available free of charge via the Internet at http://pubs.acs.org

FIGURE CAPTIONS

Figure 1. Consecutive cyclic voltammograms at 50 mVs^{-1} of Os-phendione-PVP adsorbed on spectrographic graphite: a) 2^{nd} scan; b) 50^{th} scan. In deoxygenated. In 0.1 M phosphate buffer, pH 6.0.

Figure 2. Cyclic voltammetry of an electrode modified with Os-phendione-PVP: a) in buffer; b) in 2.4 mM of NADH; c) in 4.7 mM of NADH; d) in 6.9 mM of NADH. Experimental conditions: Os-

phendione-PVP coverage (1.1±0.2)x10^{-10} mol cm^{-2}; scan rate 20 mV s^{-1} , 0.1 M phosphate buffer, pH 6.0.

Figure 3. Cyclic voltammetry of: a) bare electrode in buffer; b) bare electrode in 2.4 mM of NADH; c) electrode modified with Os-phendione-PVP (surface coverage (1.1±0.2)x10^{-10} mol/cm^2) in buffer; d) electrode modified with Os-phendione-PVP (coverage (1.1±0.2)x10^{-10} mol/cm^2) in 2.4 mM of NADH. Experimental conditions: 0.1 M phosphate buffer deaerated with argon, pH 6.0.

Figure 4. Schematic representation of the electron transfer steps for the glucose sensor based on Os-phendione-PVP polymer, NAD^+, and glucose dehydrogenase (participating protons are not shown).

Figure 5. Cyclic voltammetry of a reagentless glucose biosensor: a) in the absence of glucose; b) in 186 mM of glucose. Experimental conditions: scan rate 2 mV s^{-1}, 0.1 M phosphate buffer deaerated with argon, pH 6.0.

Figure 6. The effect of pH on the response of glucose biosensors: (●) biosensors operating in the presence of 26 mM NAD^+; (♦) reagentless biosensors; (o) controlled electrodes prepared without GDH and studied in the presence of 26 mM NAD^+; (◊) controlled electrodes prepared with GDH, without NAD^+ and studied without NAD^+ in the sample solution; (Δ) controlled electrodes prepared without GDH and studied without NAD^+ in the sample solution. Experimental conditions: temperature 25^{o}C, glucose concentration 220 mM.

TABLES

Table I. Effect of pH on the peak width at half peak height E_{fwhm}.

PH	3.0	4.0	5.0	6.0
Oxidation E_{fwhm} (mV)	95±8	110±9	121±10	134±10
Reduction E_{fwhm} (mV)	139±9	150±9	150±10	154±10

Table II. Results of data interpretation for electrocatalysis of NADH oxidation at Os-phendione-PVP modified RDE at pH 6.0 and 5.0.

pH	$k_{[NADH]=0}$ **($M^{-1}s^{-1}$)**	K_M **(mM)**	k_{+2} **(s^{-1})**
6.0	1900±200	0.75±0.09	1.5±0.1
5.0	3400±300	0.4±0.07	1.3±0.1

REFERENCES

(1) Chenault, H. K.; Whitesides G. M. *Appl. Biochem. Biotechnol.* **1987,** *14*, 147-197.

(2) Clark, W. M. In *Oxidation-Reduction Potentials of Organic Systems*, The Williams and Wilkins Co.: Baltimore, MD, 1960.

(3) Aizawa, M.; Coughlin R. W.; Charles, M. *Biochim. Biophys. Acta* **1975**, *385*, 362-370.

(4) Gorton, L. J. *Chem. Soc., Faraday Trans.* **1986**, *82*, 1245-1258.

(5) Katakis, I.; Domínguez E. *Mikrochim. Acta* **1997**, *126*, 11-32.

(6) Blaedel, W. J.; Jenkins R. A. *Anal. Chem*. **1976**, *48*, 1240-1247.

(7) Tse, D. C. S.; Kuwana, T. *Anal. Chem.* **1978**, *50*, 1315-1318.

(8) Huck, H.; Schmidt, H.L. *Angew. Chem.* **1981,** *93*, 421-422.

(9) Gorton L.; Torstensson A.; Jaegfeldt, H.; Johansson G. *J. Electroanal. Chem.* **1984,** *161*, 103-111.

(10) Kitani, A.; Miller L. L. *J. Am. Chem. Soc.* **1981,** *103*, 3595-3597.

(11) Kulys, J. J. *Enzyme Microb. Technol.* **1981**, *3*, 344-352.

(12) Gorton, L.; Johansson, G.; Torstensson, A. *J. Electroanal. Chem.* **1985**, *196*, 81-92.

(13) Goss C. A.; Abruña H. D. *Inorg. Chem.* **1985**, *24*, 4263-4267.

(14) Popescu, I. C.; Domínguez, E.; Narváez, A.; Pavlov, V.; Katakis, I. *J.* Electroanal. Chem. **1999**, *464*, 208-214.

(15) Murray, R. (Ed.), In *Molecular Design of Electrode Surfaces*, Wiley: New York, 1992.

(16) Atta, N. F.; Galal, A.; Karagözler, A. E.; Zimmer, H.; Rubinson, J. F.; Mark, H. B. *J. Chem. Soc., Chem. Commun.* **1990**, 1347-1349.

(17) Ohsaka, T.; Tanaka, T.; Tokuda, K. *J. Chem. Soc., Chem. Commun.* **1993**, 222-224.

(18) Pariente, F.; Lorenzo, E.; Abruña, H. D. *Anal. Chem.* **1994**, *66*, 4337-4344.

(19) Degrand, C.; Miller, L. L. *J. Am. Chem. Soc.* **1980**, *102*, 5728-5732.

(20) Domínguez, E.; Lan, H. L.; Okamato, Y.; Hale, P. D.; Skotheim, T. A.; Gorton, L. *Biosens. Bioelectron*. **1993**, *8*, 167-175.

(21) Persson, B.; Lee, H. S.; Gorton, L.; Skothein, T.; Bartlett, P. *Electroanalysis*, **1995**, *7*, 935-940.

(22) Parellada, J.; Narváez, A.; Domingúez, E.; Katakis, I. *Biosens. Bioelectron.* **1997**, *12*, 267-275.

(23) Evans, D. H.; Griffith, D. A. *J. Electroanal.Chem.* **1981**, *134*, 301-310.

(24) Eckert, T. S.; Bruice, T. C.; Gainor, J. A.; Weinreb, S. M. *Proc. Natl. Acad. Sci. USA* **1982**, *79*, 2533-2536.

(25) Chenault, H. K.; Whitesides, G. M. *Appl. Biochem. Biotechnol.* **1987**, *14*, 147-197.

(26) Laviron, E. *J. Electroanal. Chem.* **1980**, *109*, 57-67.

(27) Laviron, E. *J. Electroanal. Chem.* **1984**, *164*, 213-227.

(28) Laviron, E. *J. Electroanal. Chem.* **1979**, *101*, 19-28.

(29) Pauly, H. E.; Pfleiderer, G. *Hoppe-Seylers's Z. Physiol. Chem.* **1975**, *356*, 1613-1623.

(30) Albery, W. J.; Bartlett, P. N.; Cass, E. G. A.; Sim, K. W. *J. Electroanal. Chem.* **1987**, *218*, 127-134.

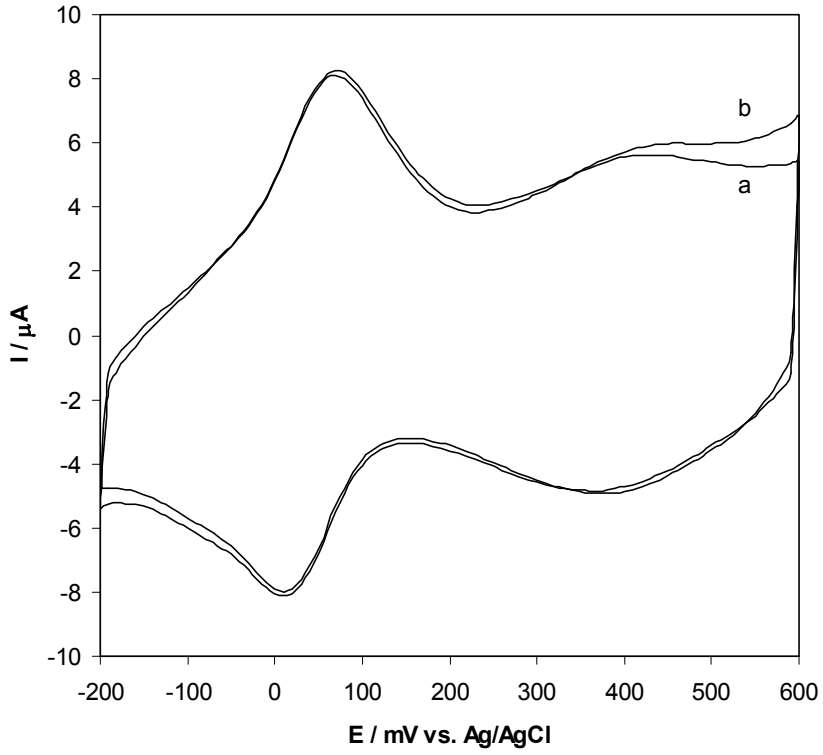
10
8
6
4
2
0
-2
-4
-6
-8
-10
-200
-100
0
100
200
300
400
500
600
I / μA
E / mV vs. Ag/AgCl
b
a

Figure 1

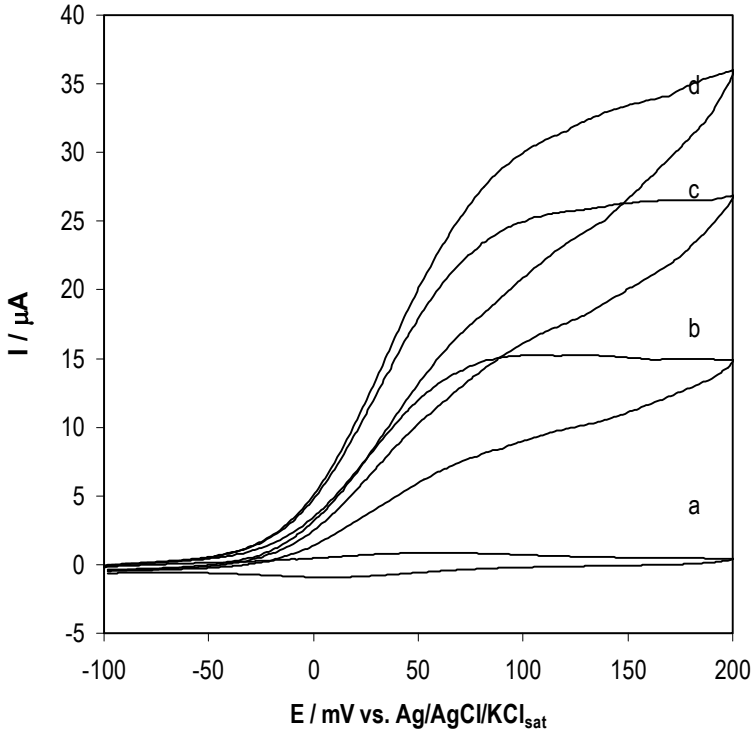
40
35
30
25
20
15
10
5
0
-5
-100
-50
0
50
100
150
200
I / μA
E / mV vs. Ag/AgCl/KCl$_{sat}$
a
b
c
d

Figure 2

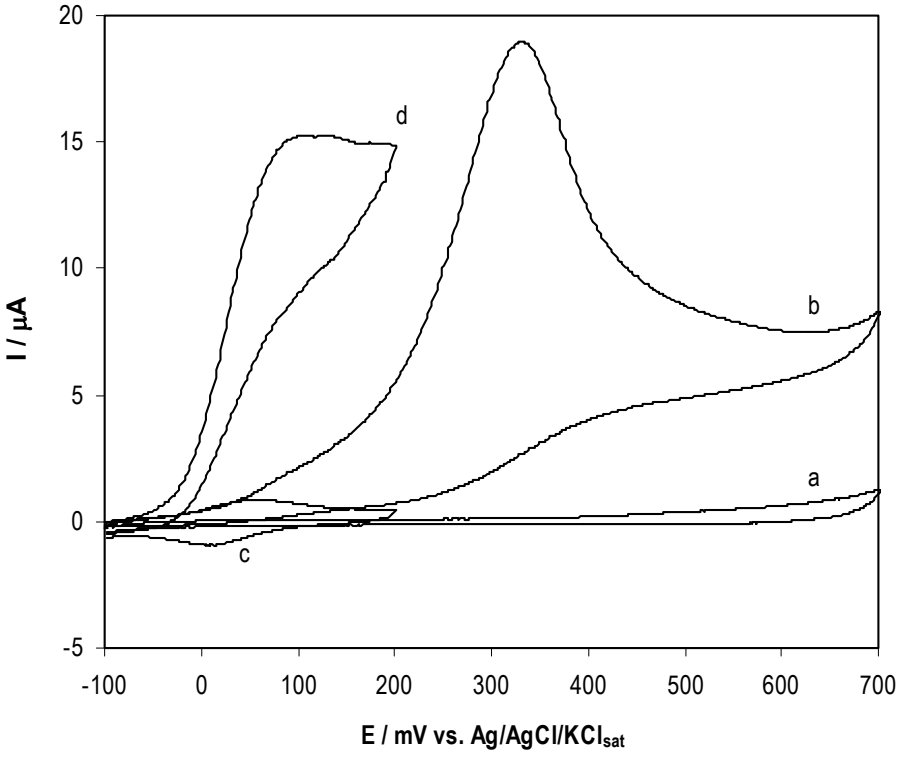
20
15
10
5
0
-5
I / µA
-100
0
100
200
300
400
500
600
700
E / mV vs. Ag/AgCl/KCl$_{sat}$
a
b
c
d

Figure 3

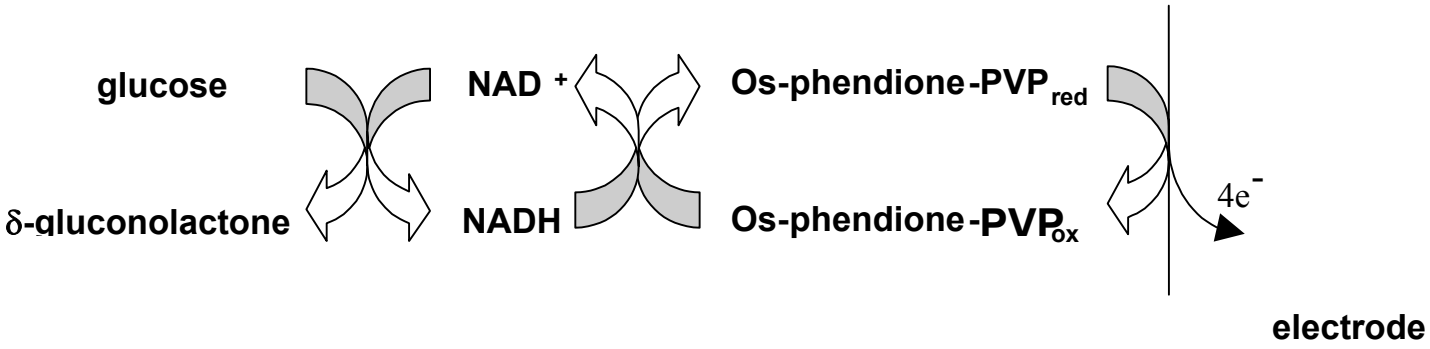
glucose
δ-gluconolactone
NAD +
NADH
Os-phendione-PVP red
Os-phendione-PVP ox
4e-
electrode

Figure 4

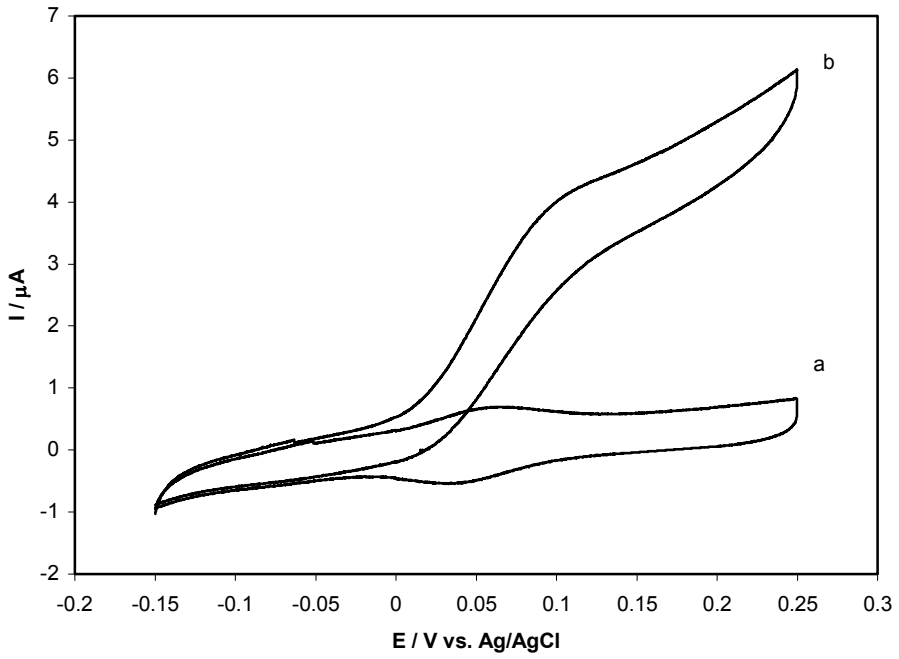
7
6
5
4
3
2
1
0
-1
-2
I / µA
b
a
-0.2
-0.15
-0.1
-0.05
0
0.05
0.1
0.15
0.2
0.25
0.3
E / V vs. Ag/AgCl

Figure 5

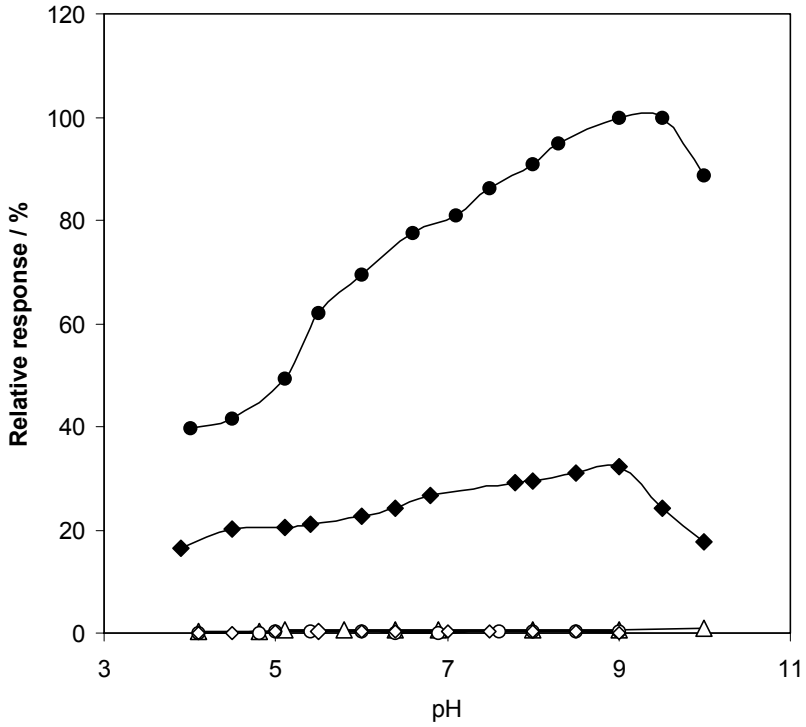

Figure 6